Transactions of the **13th International Conference on Structural Mechanics in Reactor Technology** (SMiRT 13), Escola de Engenharia - Universidade Federal do Rio Grande do Sul, Porto Alegre, Brazil, August 13-18, 1995

Effects of material and loading variables on fatigue life of carbon and low-alloy steels in LWR environments

Chopra, O.K., Shack, W.J.
Argonne National Laboratory, Argonne, Illionois, U.S.A.

ABSTRACT: The ASME Boiler and Pressure Vessel Code provides rules for the construction of nuclear power plant components. Section III of the Code specifies fatigue design curves for structural materials. While effects of reactor coolant environments are not explicitly addressed by the design curves, test data suggest that the Code fatigue curves may not always be adequate in coolant environments. This paper reports the results of recent fatigue tests that examine the effects of steel type, strain rate, dissolved oxygen level, strain range, loading waveform, and surface morphology on the fatigue life of A106–Gr B carbon steel and A533–Gr B low–alloy steel in water.

1 INTRODUCTION

The ASME Boiler and Pressure Vessel Code provides rules for the construction of nuclear power plant components in the United States. Figure I–90 of Appendix I to Section III of the Code specifies fatigue design curves for structural materials. However, the Code design curves were based primarily on fatigue tests of small polished specimens in room–temperature air, and the effects of reactor coolant environments are not explicitly addressed by the design curves. Recent data on fatigue strain vs. life (S–N) illustrate potentially significant effects of light water reactor (LWR) environments on fatigue resistance of carbon and low–alloy steels (1–10). Under certain conditions of loading and environment, fatigue lives in the test environments may be a factor of ≈100 shorter than those for the same tests in air. The magnitude of decrease in fatigue life depends on material and loading variables such as sulfur level in the steel, temperature, loading strain rate, and concentration of dissolved oxygen (DO) in water. Based on existing S–N data, Argonne National Laboratory (ANL) has developed interim fatigue design curves that account for the effects of environment on fatigue life (11). A statistical model has also been developed for estimating the effects of various material and loading conditions on fatigue life of ferritic steels; results of the statistical analysis were used to estimate the probability of initiating fatigue cracking (12).

The S–N data on carbon and low–alloy steels in water, however, are somewhat limited and do not cover the range of loading conditions found in actual reactor operation. For example, the data do not extend over the range of strain rates normally encountered in service. This paper presents experimental data under conditions where information is lacking in the existing S–N data base. Low–cycle fatigue tests have been conducted on A106–Gr B carbon steel and A533–Gr B low–alloy steel. The chemical compositions of the two materials are given in Table 1. A detailed description of the test facility and test procedure has been presented elsewhere (2). The influence of steel type, surface mor-

*Work supported by the Office of Nuclear Regulatory Research, U.S. Nuclear Regulatory Commission, under FIN Number A2212; Program Manager: Dr. M. McNeil.

Table 1. Chemical composition (wt.%) of ferritic steels used for fatigue tests

Material	Source	C	P	S	Si	Fe	Cr	Ni	Mn	Mo
A106–Gr B[a]	ANL	0.29	0.013	0.015	0.25	Bal	0.19	0.09	0.88	0.05
	Supplier	0.29	0.016	0.015	0.24	Bal	–	–	0.93	–
A533–Gr B[b]	ANL	0.22	0.010	0.012	0.19	Bal	0.18	0.51	1.30	0.48
	Supplier	0.20	0.014	0.016	0.17	Bal	0.19	0.50	1.28	0.47

[a] Schedule 140 pipe, 508–mm O.D., fabricated by Cameron Iron Works, Heat J–7201.

[b] Hot–pressed plate, 162 mm thick, from Midland reactor lower head. Austenitized at 871–899°C for 5.5 h and brine quenched, then tempered at 649–663°C for 5.5 h and brine quenched. The inner surface was inlaid with 4.8–mm weld cladding and stress relieved at 607°C for 23.8 h.

phology, applied strain range, strain rate, DO, and loading waveform on fatigue life of these steels is discussed.

2 AIR ENVIRONMENT

The fatigue data and best–fit S–N curves for A106–Gr B and A533–Gr B steels in air at 288°C are shown in Fig. 1. Fatigue life is defined as the number of cycles N_{25} for tensile stress to drop 25% from its peak value; this corresponds to a ≈3–mm deep crack in the test specimen. Results from other investigations (6,8) on similar steels with comparable composition, in particular sulfur content, and the ASME mean–data curves for carbon and low–alloy steels are also included in the figures.

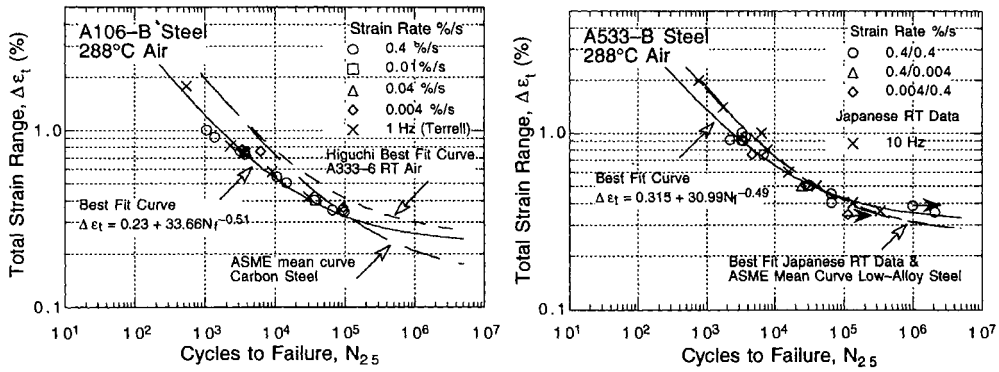

Figure 1. Total strain range vs. fatigue life data for A106–Gr B carbon steel and A533–Gr B low–alloy steel in air

The results indicate that the fatigue life of A106–Gr B carbon steel is a factor of ≈1.5 lower than that of A533–Gr B low–alloy steel. For both steels, strain rate has no effect on fatigue life in air. The data for A106–Gr B steel are in good agreement with results obtained by Terrell (6) on A106–Gr B steel, but are lower by a factor of ≈5 than those obtained by Higuchi and Iida (8) on A333–Gr 6 steel in room–temperature (RT) air. Furthermore, the data for A106–Gr B steel are below the ASME mean curve for carbon steel at high strain ranges (by a factor of 3), but are above the mean curve at low strain ranges. The results for A533–Gr B steel show good agreement with the ASME mean–data curve for low–alloy steel and the Japanese data on A533–Gr B steel compiled in the JNUFAD* data base for "Fatigue Strength of Nuclear Plant Component."

These results are consistent with the existing fatigue S–N data for carbon and low–alloy steels. A rigorous statistical analysis (12) of the available data indicates that in an air environment, the fatigue S–N curves for carbon and low–alloy steels are expressed as

*Private communication from M. Higuchi, Ishikawajima–Harima Heavy Industries Co., Japan, to M. Prager of Pressure Vessel Research Council, 1992.

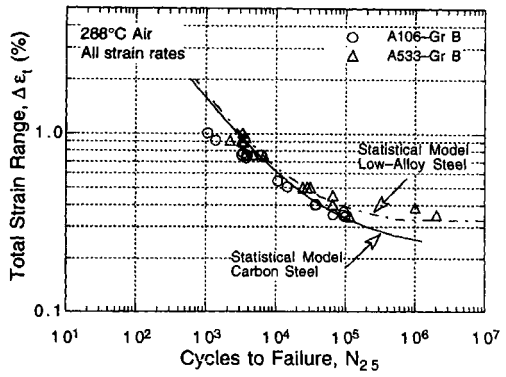

Figure 2.
Experimental and predicted fatigue lives of carbon and low–alloy steels in air

(1a) $$\ln(N_{25}) = 6.570 - 1.871\ln(\varepsilon_a - 0.11) - 0.00133T$$

(1b) and $$\ln(N_{25}) = 6.667 - 1.687\ln(\varepsilon_a - 0.15) - 0.00133T,$$

respectively, where ε_a is the strain amplitude (%) and T is temperature (°C). The experimental values of fatigue life of A106–Gr B and A533–Gr B steels in air and those predicted from Eqs. 1a and 1b are shown in Fig. 2. The predicted fatigue lives show good agreement with the experimental data.

3 ALLOY COMPOSITION

Carbon or low–alloy steel specimens develop similar surface oxide films either in air or in oxygenated water environments. In general, the specimens tested in air show slight discoloration, while the specimens tested in oxygenated water develop a gray/black corrosion scale and are covered with surface deposits. X–ray diffraction analysis of the surfaces indicated that for both steels, the corrosion scale is primarily magnetite (Fe_3O_4) in simulated pressurized water reactor (PWR) water but may also contain some hematite (Fe_2O_3) after exposure to high–DO water. Crack propagation behavior is different for the two steels. In the carbon steel, fatigue cracks propagate preferentially along the soft ferrite grains. The low–alloy steel exhibits a typical straight fatigue crack propagating normal to the stress axis.

The cyclic–hardening behaviors of the two steels are also different but are consistent with their microstructures. The A106–Gr B steel, with a pearlitic structure and low yield stress, exhibits rapid hardening during the initial 100 cycles of fatigue life. The extent of hardening increases with applied strain range. In contrast, the A533–Gr B low–alloy steel consists of a tempered bainitic structure, has a relatively high yield stress, and shows little or no initial hardening. At low strain ranges, the A533–Gr B steel shows cyclic softening during the initial 100 cycles of fatigue life. Furthermore, the A106–Gr B carbon steel exhibits dynamic strain aging. Consequently, cyclic stress of carbon steel increases significantly with decreasing strain rate. Because of its tempered bainitic structure, the low–alloy steel exhibits little or no dynamic strain aging.

The cyclic stress vs. strain curves for A106–Gr B and A533–Gr B steels at 288°C are shown in Fig. 3; cyclic stress corresponds to the value at half life. For water environment, only the tests that exhibit a marginal (≈factor of 2) decrease in fatigue life, e.g., tests in simulated PWR environment or in high–DO water at high strain rates, are shown in Fig. 3. As discussed in the next section, in high–DO water and slow strain rates, the specimens fail before the onset of dynamic strain aging and, for these tests, cyclic stresses at half life are significantly lower than that for the other tests. The results for A106–Gr B steel show excellent agreement with the data obtained by Terrell (6,7). Total strain range $\Delta\varepsilon_t$ (%) can be expressed in terms of the cyclic stress range (MPa) and strain rate $\dot{\varepsilon}$ (%/s) with the equation

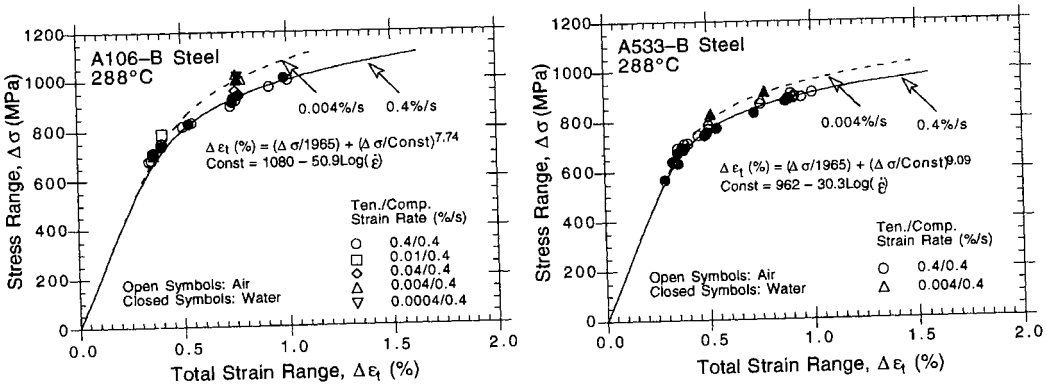

Figure 3. Cyclic stress–strain curve for A106–Gr B and A533–Gr B steels at 288°C in air and water environments

(2a) $$\Delta\varepsilon_t = \frac{\Delta\sigma}{1965} + \left(\frac{\Delta\sigma}{C}\right)^{7.74},$$

(2b) where $$C = 1080 - 50.9\mathrm{Log}(\dot{\varepsilon}).$$

The best–fit curve for A533–Gr B steel can be represented with the equation

(3a) $$\Delta\varepsilon_t = \frac{\Delta\sigma}{1965} + \left(\frac{\Delta\sigma}{D}\right)^{9.09},$$

(3b) where $$D = 962 - 30.3\mathrm{Log}(\dot{\varepsilon}).$$

4 SIMULATED PWR ENVIRONMENT

Figure 4 shows the fatigue S–N plots for A106–Gr B and A533–Gr B steels in simulated PWR water containing <10 ppb DO, 1000 ppm boron, and 2 ppm lithium. Consistent with the existing fatigue S–N data, the results indicate only a marginal effect of PWR water on fatigue life. At strain ranges >0.5%, fatigue lives of both steels in PWR water are lower than those in air by a factor of less than 2; environment has no effect on fatigue life at <0.5% strain ranges. Furthermore, a decrease in the strain rate by three orders of magnitude does not cause an additional decrease in fatigue life. The results for A106–Gr B steel are consistent with the data obtained by Terrell (7) in simulated PWR water where little or no effect of strain rate or environment on fatigue life was observed.

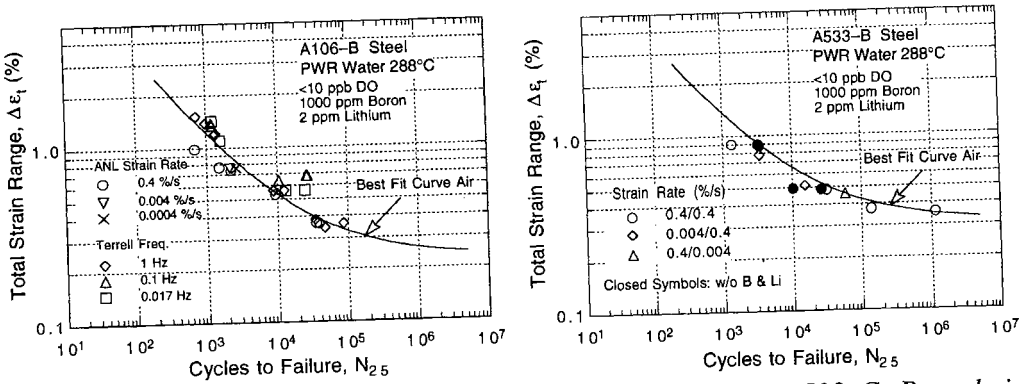

Figure 4. Strain range vs. fatigue life data for A106–Gr B and A533–Gr B steels in simulated PWR water at 288°C

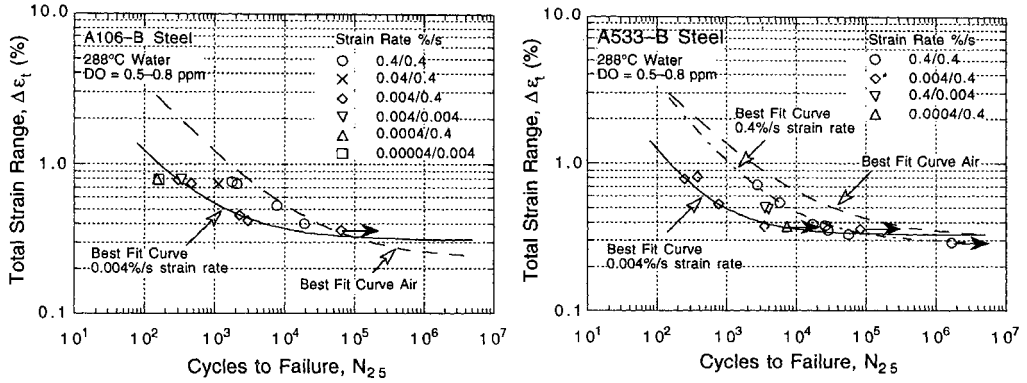

Figure 5. Total strain range vs. fatigue life data for A106–Gr B and A533–Gr B steels in high–DO water at 288°C

5 WATER WITH HIGH DISSOLVED OXYGEN

5.1 Strain Rate

The fatigue S–N plots for A106–Gr B and A533–Gr B steels in water containing 0.5–0.8 ppm DO are shown in Fig. 5. The results indicate significant reductions in fatigue life and a strong dependence on strain rate. Although the microstructures and cyclic–hardening behaviors of the A106–Gr B carbon steel and A533–Gr B low–alloy steel are significantly different, there is little or no difference in environmental degradation of fatigue life of these steels. For both steels, fatigue life decreases rapidly with decreasing strain rate. Compared with tests in air, fatigue life of A106–Gr B steel in high–DO water is lower by factors of 2, 4, 10, and 18 at strain rates of 0.4, 0.04, 0.004, and 0.0004%/s, respectively. A further decrease in strain rate to 0.00004%/s does not cause additional decrease in fatigue life. The relative reduction in fatigue life is about the same whether the total strain range is 0.75 or 0.4%.

The low–alloy A533–Gr B steel shows an identical behavior. For similar test conditions, the absolute values of fatigue life for A533–Gr B low–alloy steel are comparable to those for A106–Gr B carbon steel. However, because life in air for A533–Gr B steel is greater than that for A106–Gr B steel, the relative reduction in life for the low–alloy steel is larger than that for carbon steel. This is particularly true at low strain range (0.4%), where even at the high strain rate, fatigue life is a factor of ≈10 lower than in air. These results are different than the Japanese data compiled in the JNUFAD data base, which indicate that environmental effects on fatigue life are greater for carbon steel than for low–alloy steel. However, most low–alloy steels that have been investigated in JNUFAD are low–sulfur heats, e.g., <0.007 wt.%. It is likely that differences between these two steels in JNUFAD data base are caused by the sulfur content of the steels and that compositional or structural differences have only minor effects. The sulfur content of ANL heats of A106–Gr B and A533–Gr B steel is comparable.

The results presented in Fig. 5 also indicate that a slow strain rate applied during the tensile–loading cycle (slow/fast test) is more effective in environmentally assisted reduction in fatigue life than when applied during the compressive–loading cycle (fast/slow test), and that slow strain rate applied during the compressive– and tensile–loading cycles (slow/slow test) does not cause further decrease in fatigue life. Two fatigue tests on A106–Gr B steel at a strain range of ≈0.75%, one with a slow/fast waveform (i.e., 0.004 and 0.4%/s strain rates, respectively, during the tensile and compressive half of the loading cycle) and the other with a slow/slow waveform (i.e., 0.004%/s constant strain rate), show identical fatigue lives. However, two fatigue tests on A533–Gr B steel at ≈0.5% strain range and fast/slow waveform (shown as inverted triangles in Fig. 5) do show a somewhat larger decrease in fatigue life than for a fast/fast test, viz., a

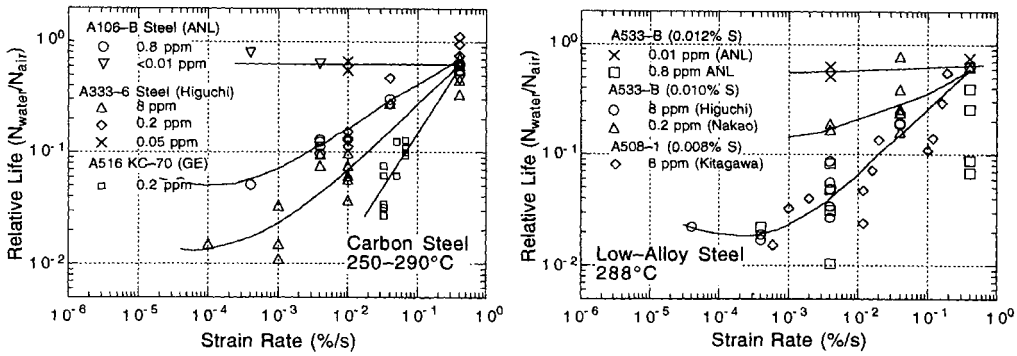

Figure 6. Relative fatigue life of several heats of carbon and low–alloy steels at different levels of dissolved oxygen and strain rate

factor of 8 decrease in life for the fast/slow test, compared to a factor of 5 decrease for the fast/fast test.

The relative fatigue lives of several heats of carbon and low–alloy steels are plotted as a function of strain rate in Fig. 6. Relative fatigue life is the ratio of life in water to life of that specific heat in air. The results indicate that in addition to the dependence on strain rate, environmental effects on fatigue life of carbon and low–alloy steels may also depend on DO level in water and sulfur content in the steel. Fatigue life of these steels in high–DO water decreases with decreasing strain rates and increasing levels of DO and sulfur. The effect of strain rate on fatigue life appears to saturate at ≈0.001%/s strain rate.

The very–high–sulfur A516–Gr 70 carbon steel (0.033 wt.% sulfur) from the GE tests at the Dresden 1 reactor (4) shows the most severe environmental degradation. For this steel at a given strain rate, the reduction in fatigue life at 0.2 ppm DO is greater by a factor of ≈2 than that for the A106–Gr B steel at 0.8 ppm DO and for the A333–Gr 6 steel at 0.2 ppm DO. It is unclear whether this difference is due to the extremely high sulfur level in this heat or to the loading waveform used in the Dresden tests. These tests were conducted with a trapezoidal waveform instead of the sawtooth and triangular waveforms used in the ANL and Japanese studies. The trapezoidal waveform consists of hold periods at peak tensile and compressive strains. As discussed later, a hold period at peak tensile stress also decreases fatigue life. In Fig. 6, the data points for this steel will move to the left when the contributions of the hold periods are considered.

These results have been used to develop a statistical model (12) for estimating the effects of various material and loading conditions on fatigue life of ferritic steels. In oxygenated water environments, the fatigue S–N curves for carbon and low–alloy steels are expressed as

(4a) $$\ln(N_{25}) = 6.186 - 1.871\ln(\varepsilon_a - 0.11) + 0.554S^*T^*O^*\dot{\varepsilon}^*$$

(4b) and $$\ln(N_{25}) = 5.518 - 1.687\ln(\varepsilon_a - 0.15) + 0.554S^*T^*O^*\dot{\varepsilon}^*,$$

respectively, where S^*, T^*, O^*, and $\dot{\varepsilon}^*$ are transformed sulfur content S, temperature T, DO, and strain rate $\dot{\varepsilon}$ respectively, defined as follows:

(5a) $S^* = S$ (0<S<0.015 wt.%)
$S^* = 0.015$ (S≥0.015 wt.%)

(5b) $T^* = 0$ (T<150°C)
$T^* = T–150$ (T≥150°C)

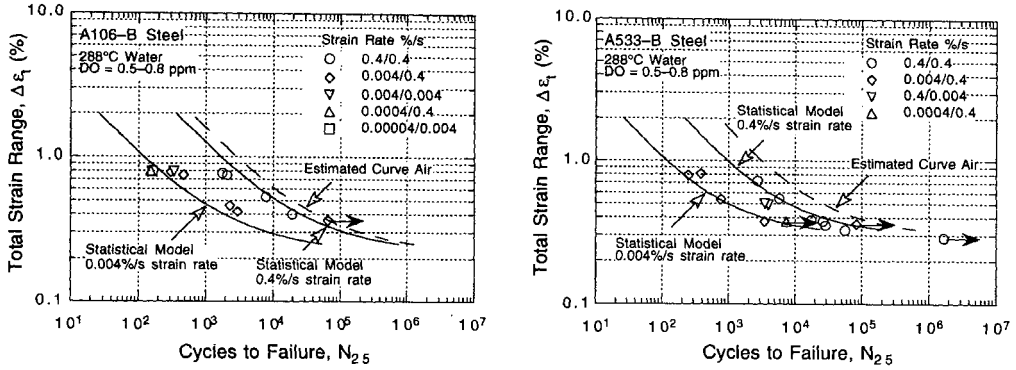

Figure 7. Experimental and predicted fatigue lives of carbon and low–alloy steels at 288°C in water containing ≥0.5 ppm dissolved oxygen

(5c) $O^* = 0$ (DO<0.05 ppm)
$O^* = DO$ (0.05 ppm≤DO≤0.5 ppm)
$O^* = 0.5$ (DO>0.5 ppm)

(5d) $\dot{\varepsilon}^* = 0$ ($\dot{\varepsilon}$>1%/s)
$\dot{\varepsilon}^* = \ln(\dot{\varepsilon})$ (0.001≤$\dot{\varepsilon}$≤1%/s)
$\dot{\varepsilon}^* = \ln(0.001)$ ($\dot{\varepsilon}$<0.001%/s)

The experimental values of fatigue life of A106–Gr B and A533–Gr B steels in high–DO water and those predicted from Eqs. 4a and 4b are shown in Fig. 7. The predicted fatigue lives show good agreement with the experimental results.

5.2 Strain Range

The fatigue data in high–DO water indicate that a minimum strain is required for environmentally assisted decrease in fatigue life. This threshold value of strain range for the ANL heats of carbon and low–alloy steels appears to be at ≈0.36%; fatigue tests on A106–Gr B and A533–Gr B steels at ≈0.36% strain range, 0.6–0.8 ppm DO, and 0.004%/s tensile strain rate did not produce failure even after 65,000 and 83,000 cycles, respectively (Fig. 5). Furthermore, the fatigue S–N curves for A106–Gr B steel in air and water environments cross over at low strain ranges, i.e., fatigue life in water is longer than that in air. This apparently different fatigue S–N behavior is probably not due to the water environment. It is most likely caused by dynamic strain aging of carbon steels and is observed in Fig. 5 because of the difference in strain rate for the tests in air and water environments. The S–N curve in air is based on tests at 0.4%/s strain rate, while the curve in water represents fatigue tests at a slower strain rate of 0.004%/s. For a specific strain range, fatigue tests in water at slower strain rate show greater dynamic strain aging, higher cyclic stress, lower plastic strain range, and longer life.

TENSILE HOLD PERIOD

Tests were also conducted with a 5– or 30–min hold at peak tensile strain. The results indicate that a tensile–hold period decreases fatigue life in high–DO water but not in air. A 5–min hold is sufficient to reduce fatigue life; a longer hold period results in only slightly decreased life. Two 5–min–hold tests at 288°C and ≈0.8% strain range in oxygenated water with 0.7 ppm DO gave fatigue lives of 1,007 and 1,092 cycles. Fatigue life in a 30–min–hold test was 840 cycles. These tests were conducted in stroke–control mode and are somewhat different than the conventional hold–time test in strain–control

mode. In the strain–control test, total strain in the sample is held constant during the hold period. However, a portion of the elastic strain is converted to plastic strain because of stress relaxation. In a stroke–control test, there is an additional plastic strain in the sample due to relaxation of elastic strain from the load train. Consequently, these are not true constant–strain–hold periods but include significant strain during the hold period; the measured plastic strains during the hold period were ≈0.028% from relaxation of the gage and 0.05–0.06% from relaxation of the load train. These conditions result in strain rates of 0.005–0.02%/s during the hold period.

SURFACE MORPHOLOGY

The fatigue crack growth behavior of ferritic steels in high–temperature oxygenated water and the effects of sulfur content and loading rate are well known (13–18). Dissolution of MnS inclusions changes the water chemistry near the crack tip, making it more aggressive. This results in enhanced crack growth rates because either (a) the dissolved sulfides decrease the repassivation rate, which increases the amount of metal dissolution for a given oxide rupture rate; or (b) the dissolved sulfide poisons the recombination of H atoms liberated by corrosion, which enhances H uptake by the steel at the crack tip.

The water environment may also enhance crack nucleation. For example, corrosion pits or cavities produced by dissolution of MnS inclusions can act as sites for nucleation of fatigue cracks (19,20). A detailed metallographic examination, including measuring the cracking frequency, of the test specimens was conducted to investigate the role of surface micropitting on fatigue crack nucleation. The results have been presented elsewhere (21). All specimens tested in water showed surface micropitting. However, metallographic examination of the specimens indicates that an oxygenated–water environment has no effect on the nucleation of cracks. There is no indication that fatigue cracks nucleated at any of the surface micropits. Irrespective of environment, cracks in carbon and low–alloy steels nucleate either along slip bands, carbide particles, or at the ferrite/pearlite phase boundaries. The results also show that environment has no effect on the frequency of cracks. For similar loading conditions, the number of cracks in the specimens tested in air and high–DO water are identical, although fatigue life in water is lower by a factor of ≈10.

The contributions of environment to crack nucleation were further evaluated by conducting additional exploratory tests. Figure 8 shows the fatigue life of A106–Gr B steel in air (dashed line) and in high–DO water at 0.4 and 0.004%/s strain rates (circle and diamond symbols, respectively). Fatigue tests were conducted on specimens that were preexposed at 288°C for 30–100 h in water with 0.6–0.8 ppm DO and then tested either in air or low–DO water (<10 ppb DO). At 0.4% strain range, nearly half the fatigue life may be spent in crack nucleation. Fatigue lives of the preoxidized specimens are identical to those of unoxidized specimens; life would be expected to decrease if surface

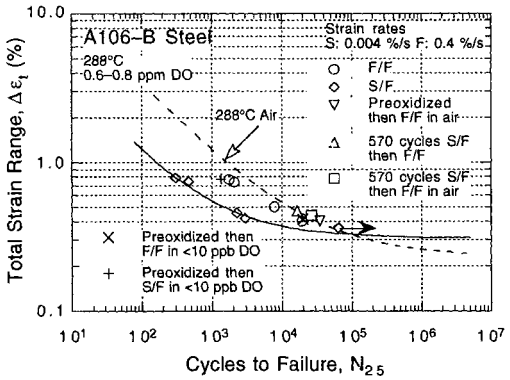

Figure 8.
Environmental effects on nucleation of fatigue crack. Preoxidized specimens were exposed at 288°C for 30–100 h in water with 0.6–0.8 ppm DO.

micropits facilitate crack nucleation. Similar behavior was observed for preoxidized A533–Gr B specimens.

It is possible that both the high DO and slow strain rate are needed to influence crack nucleation. This possibility was checked by first testing a specimen in high–DO water at 0.4% strain range and 0.004%/s strain rate for 570 cycles (≈25% of the life at these loading conditions) and then testing in either air or high–DO water at 0.4%/s strain rate. Fatigue life of these tests should be reduced if crack nucleation contributes in any way to environmental effects. Once again, no reduction in life is observed. These results suggest that the reduction in fatigue life in high–DO water is primarily due to environmental effects on fatigue crack growth. Environment appears to have little or no effect on crack nucleation.

LOADING WAVEFORM

Several exploratory tests were conducted on A106–Gr B and A533–Gr B steels in which a slow strain rate is applied during only a portion of the tensile–loading cycle to check whether each portion of the tensile cycle is equally effective in decreasing fatigue life in high–DO water. The loading waveforms and corresponding fatigue lives for the tests on A106–Gr B steel at ≈0.75% strain range are summarized in Fig. 9. The change in fatigue life of A106–Gr B steel with fraction of loading strain at slow strain rate is shown in Fig. 10. Results are shown for slow portions applied near to peak tensile strain (open symbols) or near to peak compressive strain (closed symbols). In stroke–controlled tests, the fraction of loading strain that is actually applied to the specimen gage section is not constant but varies during the cycle. Consequently, for waveforms D and H, although 0.5 of the applied displacement is at a slow rate, the fractions of strain at slow rate in the specimen gage section are 0.334 and 0.666, respectively. The fraction of loading strain that is actually at slow rate for the various waveforms is given in Fig. 9.

At 288°C and a strain range of ≈0.75%, the average fatigue life of A106–Gr B steel in air is ≈4000 cycles. Relative to air, the fatigue lives in simulated PWR water at all strain rates or in high–DO water at high strain rates (i.e., fast/fast tests) are lower by ≈50%. If each portion of the tensile–loading cycle was equally effective in reducing fatigue life, the life should decrease linearly from A to C along the chain–dot line in Fig. 10 and a slow strain rate near peak compressive strain (waveforms D, E, or F) should be as equally damaging as a slow strain rate near peak tensile strain (waveforms H, I, or J). The results show that a slow strain rate near peak compressive strain causes no reduction in fatigue life.

As was discussed above in the section on "Strain Range," a minimum amount of strain is required for environmentally assisted decrease in fatigue life. This threshold strain may vary with material and loading conditions such as steel type, temperature, DO, strain ratio, mean stress, etc. For the present study, the threshold strain range for A106–Gr B carbon steel is ≈0.36%. Consequently, a slow strain rate applied during the portion of loading cycle that is below the threshold strain should have no effect on fatigue life. This behavior is consistent with the slip–dissolution model for crack propagation (22); the applied strain must exceed a threshold value to rupture the passive surface film in order for environmental effects to occur. (Note that this need not imply that the observed threshold strain is the actual film rupture strain. The film rupture occurs at the crack tip and is controlled by the crack tip strain. The threshold strain measured in smooth–specimen tests is a surrogate that in essence controls the crack tip strain, but no numerical equality between the two need be implied). If each portion of the loading cycle above the threshold strain is equally damaging, the decrease in fatigue life should follow line ABC when slow rate is applied near peak tensile strain and line ADC when it is applied near peak compressive strain. The results are in agreement with this behavior, i.e., a slow strain rate applied during each portion of the loading cycle above the threshold strain is equally effective in decreasing fatigue life.

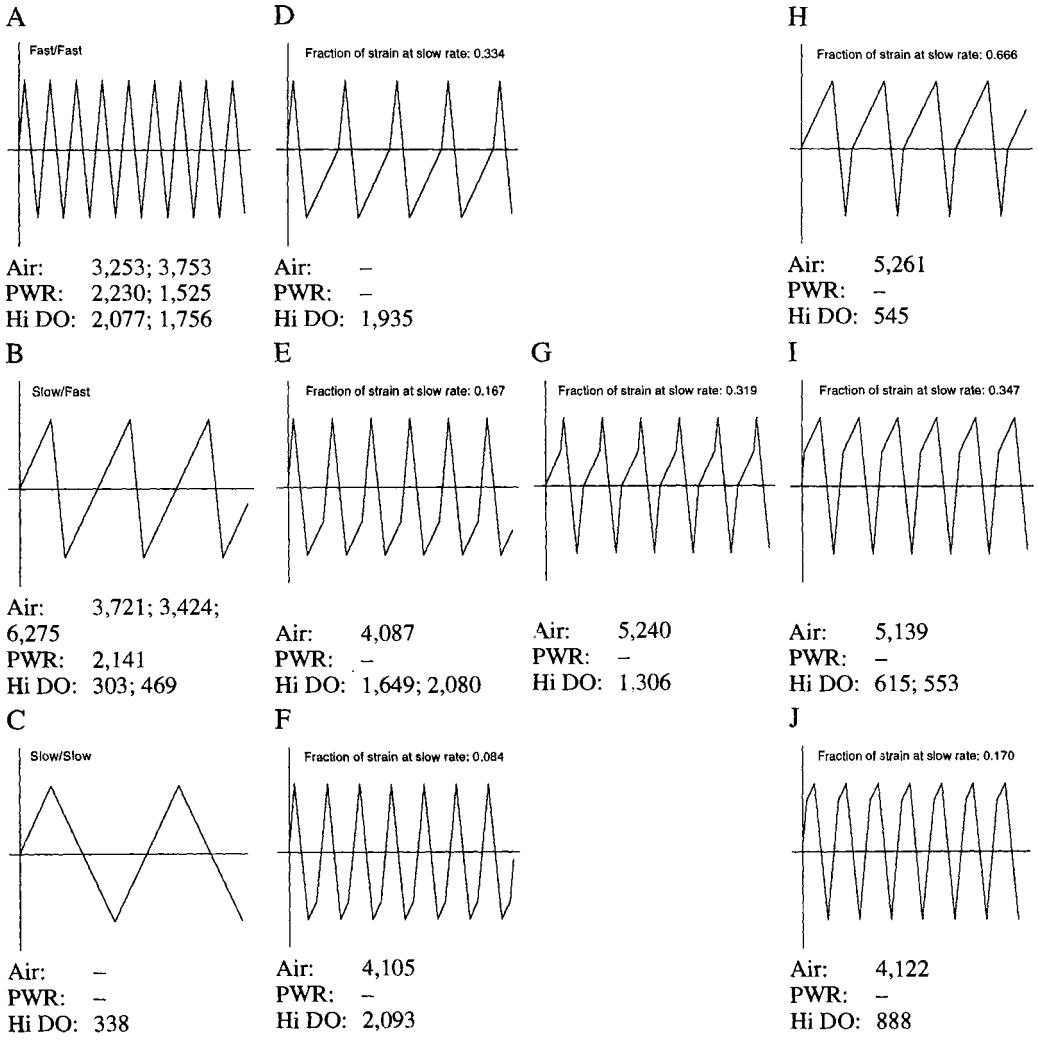

Figure 9. Fatigue life of A106–Gr B carbon steel at 288°C and 0.75% strain range in air and water environments under different loading waveforms

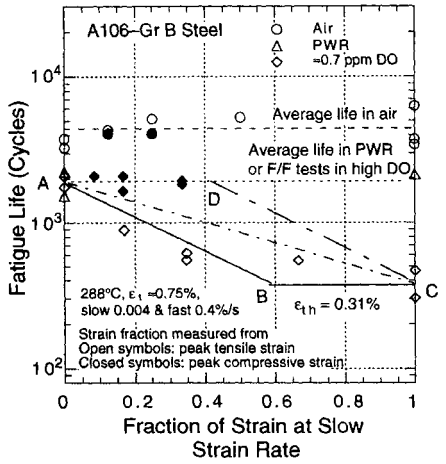

Figure 10.
Fatigue life of A106–Gr B steel tested in air and water with loading waveforms where slow strain rate is applied during a fraction of the tensile cycle.

CONCLUSIONS

Fatigue behavior of A106–Gr B carbon steel and A533–Gr B low–alloy steel has been investigated in air and water environments. The results confirm the significant reduction in fatigue life in high–DO water and strong dependence on strain rate. The results show that although the structure and cyclic–hardening behavior of carbon and low–alloy steels are distinctly different, there is little or no difference in susceptibility to environmental degradation of fatigue life of these steels when sulfur levels are comparable. The A106–Gr B carbon steel exhibits pronounced dynamic strain–aging, whereas strain–aging effects are modest in the A533–Gr B low–alloy steel.

For both steels, the results indicate only a marginal effect of simulated PWR environment on fatigue life, e.g., fatigue life is lower by less than a factor of 2 than that in air. Furthermore, fatigue life is independent of strain rate; a three–order–of–magnitude decrease in strain rate does not cause an additional decrease in life.

Environmental effects on fatigue life are significant at high DO levels, e.g., 0.5–0.8 ppm DO. In high–DO water, the effects of various loading and environmental parameters on fatigue life of carbon and low–alloy steels are summarized below.

(i) The fatigue life of carbon and low–alloy steels decreases rapidly with decreasing strain rate. For both steels, the effect of strain rate saturates at ≈0.001%/s.

(ii) A minimum strain is required for environmentally assisted decrease in fatigue life. For the loading conditions used in the present study, this threshold strain range appears to be ≈0.36% for the heats of carbon and low–alloy steels investigated.

(iii) A slow strain rate applied during the tensile–loading cycle is more effective in environmentally assisted reduction in fatigue life than applied during the compressive–loading cycle.

(iv) The results also indicate that a slow strain rate applied during each portion of the tensile–loading cycle above the minimum threshold strain is equally effective in decreasing fatigue life.

(v) A hold period at peak tensile strain decreases fatigue life in high–DO water but not in air. A 5–min hold is sufficient to reduce fatigue life.

(vi) The results indicate that the reduction in fatigue life in high–DO water is primarily due to environmental effects on fatigue crack growth. Although all specimens tested in water show surface micropitting, there is no indication that these micropits enhance crack nucleation. Irrespective of environment, cracks in carbon and low–alloy steels nucleate either along slip bands, carbide particles, or at the ferrite/pearlite phase boundaries.

REFERENCES

1. Hicks, P. D. & W. J. Shack. 1992. Fatigue of Ferritic Steels. In *Environmentally Assisted Cracking in Light Water Reactors, Semiannual Report, April–September 1991*, NUREG/CR–4667 Vol. 13, ANL–92/6, pp. 3–8.
2. Chopra, O. K., W. F. Michaud & W. J. Shack. Fatigue of Ferritic Steels. 1993. In *Environmentally Assisted Cracking in Light Water Reactors, Semiannual Report, October 1992–March 1993*, NUREG/CR–4667 Vol. 16, ANL–93/27, pp. 3–19.
3. Chopra, O. K. & W. J. Shack. 1995 Effects of LWR Environments on Fatigue Life of Carbon and Low–Alloy Steels. In Proc. 1995 ASME/JSME Pressure Vessel and Piping Conference, July 23-27, Hawaii.
4. Hale, D. A., S. A. Wilson, E. Kiss & A. J. Gianuzzi. 1977. Low Cycle Fatigue Evaluation of Primary Piping Materials in a BWR Environment. GEAP–20244, U.S. Nuclear Regulatory Commission.
5. Ranganath, S., J. N. Kass, & J. D. Heald. 1982. Fatigue Behavior of Carbon Steel Components in High–Temperature Water Environments. In C. Amzallag, B. N. Leis,

and P. Rabbe (eds.), *Low–Cycle Fatigue and Life Prediction*, ASTM STP 770, pp. 436–459, American Society for Testing and Materials, Philadelphia.

6. Terrell, J. B. 1988. Fatigue Life Characterization of Smooth and Notched Piping Steel Specimens in 288°C Air Environments. NUREG/CR–5013, MEA–2232.
7. Terrell, J. B. 1988. Effect of Cyclic Frequency on the Fatigue Life of ASME SA–106–B Piping Steel in PWR Environments. *J. Mater. Eng.* 10:193–203.
8. Higuchi, M. & K. Iida. 1991. Fatigue Strength Correction Factors for Carbon and Low–Alloy Steels in Oxygen–Containing High–Temperature Water. *Nucl. Eng. Des.* 129:293–306.
9. K. Iida, H. Kobayashi & M. Higuchi. 1986. Predictive Method of Low Cycle Fatigue Life of Carbon and Low Alloy Steels in High Temperature Water Environments. NUREG/CP–0067, MEA–2090, Vol. 2.
10. Nagata, N., S. Sato & Y. Katada. 1989. Low–Cycle Fatigue Behavior of Low–Alloy Steels in High–Temperature Pressurized Water. In A. H. Hadjian (ed.), *Transactions of the 10th International Conf. on Structural Mechanics in Reactor Technology,*. American Association for Structural Mechanics in Reactor Technology, Anaheim, CA.
11. Majumdar, S., O. K. Chopra & W. J. Shack. 1993. Interim Fatigue Design Curves for Carbon, Low–Alloy, and Austenitic Stainless Steels in LWR Environments. NUREG/CR–5999, ANL–93/3.
12. Kiesler, J. & O. K. Chopra. 1995. Statistical Analysis of Fatigue Strain–Life Data for Carbon and Low–Alloy Steels. In Proc. 1995 ASME/JSME Pressure Vessel and Piping Conference, July 23-27, Hawaii.
13. Speidel, M. O. & R. M. Magdowski. 1988. Stress Corrosion Cracking of Nuclear Reactor Pressure Vessel Steel in Water: Crack Initiation versus Crack Growth. *Corrosion 88*. Paper No. 283.
14. Ford, F. P. & P. L. Andresen. 1990. Stress Corrosion Cracking of Low–Alloy Pressure Vessel Steel in 288°C Water. In *Proc. 3rd Int. Atomic Energy Agency Specialists' Meeting on Subcritical Crack Growth.* NUREG/CP–0112 Vol. 1, pp. 37–56.
15. Scott, P. M. & D. R. Tice. 1990. Stress Corrosion in Low–Alloy Steels. *Nucl. Eng. Des.* 119:399–413.
16. Van Der Sluys, W. A. & D. S. DeMiglio. 1983. An Investigation of Fatigue Crack Growth in SA508–2 in a 288°C PWR Environment by a Constant ΔK Test Method. In *Proc. Int. Atomic Energy Agency Specialists' Meeting on Subcritical Crack Growth.* NUREG/CP–0044, MEA–2014 Vol. 1, pp. 44–64.
17. Bulloch, J. H. 1989. A Review of the Fatigue Crack Extension Behavior of Ferritic Pressure Vessel Materials in Pressurized Water Reactor Environments. *Res. Mechanica.* 26:95–172.
18. Kassner, T. F., W. J. Shack, W. E. Ruther, & J. H. Park. 1991. Environmentally Assisted Cracking of Ferritic Steels. In *Environmentally Assisted Cracking in Light Water Reactors: Semiannual Report, April–September 1990.* NUREG/CR–4667, Vol. 11, ANL–91/9, pp. 2–9.
19. Macdonald, D. D., S. Smialowska & S. Pednekar. 1983. The General and Localized Corrosion of Carbon and Low–Alloy Steels in Oxygenated High–Temperature Water. NP–2853.
20. Kuniya, J., H. Anzai & I. Masaoka,. 9192. Effect of MnS Inclusions on Stress Corrosion Cracking in Low–Alloy Steels. *Corrosion.* 48 (5):419–425.
21. Chopra, O. K., W. F. Michaud & W. J. Shack. 1994. Fatigue of Ferritic Steels. In *Environmentally Assisted Cracking in Light Water Reactors, Semiannual Report, March 1993–April 1994.* NUREG/CR–4667 Vol. 17, ANL–94/16, pp. 1–22.
22. Ford, F. P., S. Ranganath & D. Weinstein,. 1993. Environmentally Assisted Fatigue Crack Initiation in Low–Alloy Steels – A Review of the Literature and the ASME Code Design Requirements. EPRI Report TR–102765.